

Bimetallic Reactivity. Oxidative-Addition and Reductive-Elimination Reactions of Rhodium and Iridium Bimetallic Complexes

TERRY G. SCHENCK, C. R. C. MILNE, J. F. SAWYER, and B. BOSNICH*

Received September 12, 1984

Homobimetallic complexes of rhodium(I) and iridium(I) containing the binucleating ligand PNNP undergo oxidative-addition and reductive-elimination reactions with acetyl chloride and methyl iodide. Depending on the electron richness of the metals, a complete spectrum of possibilities is observed from reversible single oxidative addition on one of the metals to irreversible double oxidative addition on both metals. Oxidative addition to one metal leads to deactivation of the other metal despite the fact that no metal-metal bonds are formed. A crystal structure of a rhodium(I)-rhodium(III) complex $[\text{Rh}_2(\mu\text{-PPh}_2)(\text{CO})_2\text{PNNP}(\text{CH}_3)\text{I}]\cdot\text{C}_4\text{H}_{10}\text{O}$ has been determined and shows the two metals to be separated by 3.766 Å. Crystals are triclinic, space group $P\bar{1}$, $a = 12.211$ (4) Å, $b = 13.313$ (7) Å, $c = 15.616$ (7) Å, $\alpha = 79.34$ (5)°, $\beta = 72.64$ (3)°, $\gamma = 84.37$ (4)°, $V = 2379$ Å³, $D_{\text{calcd}} = 1.57$ g cm⁻³ for $Z = 2$, and $R = 0.0401$ for 6739 observed ($I > 3\sigma(I)$) reflections. The bis(diene) species of rhodium and iridium are precursors for catalytic hydrogenation of alkenes and alkynes.

One of the more interesting current endeavors is the synthesis of multimetallic transition-metal complexes in which the metals are held at specific distances from each other. Such systems, through cooperative electronic and/or steric effects between metal centers, might give rise to distinct reactivity patterns for both their stoichiometric and catalytic reactions which are not available to their monometallic analogues. Most multimetallic systems described so far are capable of metal-metal bond formation, and some of the more interesting reactions of these systems are connected with the making and breaking of these metal-metal bonds. It seemed to us useful to design a rigid bimetallic system in which the metals were within cooperative distance but were incapable of forming metal-metal bonds. In this way we hoped to identify the effect of metal-metal bond formation on the reactivities of bimetallic systems.

In the preceding paper¹ we described a new family of bimetallic palladium, rhodium, and iridium complexes having the desired structural characteristics. These complexes incorporated the quadridentate (linked bis bidentate) binucleating ligand, PNNP (Figure 1). We document here some of our results on the stoichiometric and catalytic reactivities of the rhodium and iridium complexes.

1. Catalytic Hydrogenation. The homogenous hydrogenation of unsaturated substrates using mononuclear complexes of the type $[\text{M}(\text{diene})\text{L}_2]^+$ ($\text{M} = \text{Rh},^{2-4} \text{Ir}^5$) has been extensively investigated. This allowed us to compare these results with those we obtained using the analogous bimetallic precursors $[\text{Rh}_2(\text{NBD})_2\text{PNNP}]\text{BF}_4$ (2) and $[\text{Ir}_2(\text{COD})_2\text{PNNP}]\text{BF}_4\cdot\text{CH}_3\text{OH}$ (4) (Figure 1). The results of the bimetallic hydrogenations are summarized in Table I. A comparison of the data in Table I with those reported for the mononuclear counterparts reveals that there are certain differences between the two. For example, it has been observed that in polar solvents, $[\text{Ir}(\text{diene})\text{L}_2]^+$ complexes are very poor hydrogenation catalysts compared with the corresponding rhodium analogues.² In nonpolar solvents this dichotomous behavior does not prevail, and both the rhodium and iridium mononuclear complexes are very active hydrogenation catalysts.⁵ The data in Table I, which refer to methanol as solvent, indicate that this deactivation of the iridium species does not occur for the bimetallic complexes. The reduction of alkynes catalyzed by $[\text{Rh}(\text{NBD})\text{diphos}]^+$ is reported to proceed with high selectivity to yield 98% *cis*-alkene products.^{2,3} The bimetallic rhodium and iridium catalysts appear to be less selective, yielding mixtures of *cis*-stilbene (75%), *trans*-stilbene (12%), and dibenzyl (12%) from

diphenylacetylene. The hydrogenation of 1,3-cyclohexadiene catalyzed by $[\text{Rh}_2(\text{NBD})_2\text{PNNP}]^+$ results in a rapid disproportionation to a 1:1 mixture of benzene and cyclohexene followed by a slower reduction of the produced cyclohexene to cyclohexane. Mononuclear rhodium complexes that have been shown to catalyze this disproportionation include $[\text{Rh}(\text{NBD})_2]^+{}^6$ and $[\text{Rh}(\text{NBD})(\text{P}(\text{CH}_3)_2\text{Ph})_2]^+{}^4$ although with the chelating phosphine complex $[\text{Rh}(\text{NBD})\text{diphos}]^+$ direct hydrogenation of 1,3-cyclohexadiene to cyclohexene and then to cyclohexane occurs.⁴ Finally, there were several substrates (Table I) that were not reduced by either of the $[\text{M}_2(\text{diene})_2\text{PNNP}]^+$ complexes. These substrates, which are potential bidentate ligands, may form sufficiently stable complexes that may lead to catalyst deactivation although their reduction by $[\text{Rh}(\text{NBD})\text{diphos}]^+$ is reported to occur efficiently.^{3,4}

Thus, the $[\text{M}_2(\text{diene})_2\text{PNNP}]^+$ complexes show some similarities as well as some significant differences in their catalytic activity compared to the mononuclear analogues. The bimetallic complexes appear to accept a limited variety of substrates for reduction and are less selective (cf. diphenylacetylene). We have looked more closely at the hydrogenation process for these bimetallic substrates.

When solutions (CH_3OH , THF, CH_2Cl_2) of either $[\text{M}_2(\text{diene})_2\text{PNNP}]^+$ complex are treated with hydrogen at ambient conditions, dark red solutions result. The ¹H NMR spectra of these solutions show that the diene has been reduced completely. The signals associated with the PNNP ligand are broad and featureless, and no metal hydride signals were detected, suggesting that oligomeric complexes may have been formed. Addition of more diene to these dark red solutions does not result in the regeneration of the starting diene complexes. We have been unable to isolate any well-defined complexes from these solutions.

If, however, an orange solution of $[\text{Ir}_2(\text{COD})_2\text{PNNP}]\text{BF}_4\cdot\text{C}_4\text{H}_9\text{OH}$ is exposed to hydrogen at -78 °C, the solution turns pale yellow and gives a well-defined ¹H NMR spectrum. The metal hydride region of such a spectrum is shown in Figure 2. The two, equally intense hydride resonances at δ -9.00 and -18.59 display chemical shifts and coupling constants in agreement with an octahedral iridium(III) center bearing one *cis* (to phosphorus) and one *trans* (to phosphorus) metal hydride ligand.⁷ The COD ligands remain on the complex, and their integrated ¹H NMR signals compared to the metal hydride signals reveals that only 1 equiv of H₂ has added to the bimetallic unit. When this solution is warmed to -10 °C, the original orange color is restored and the ¹H NMR spectrum is the same as that of the starting $[\text{Ir}_2(\text{COD})_2\text{PNNP}]^+$ complex. Thus, the addition of hydrogen is reversible at these low temperatures and occurs on only one metal center of the bimetallic complex (Figure 3). Presumably during hydrogenation of the COD ligand at 25 °C, the hydrogen oxi-

(1) Schenck, T. G.; Downes, J. M.; Milne, C. R. C.; Mackenzie, P. B.; Boucher, B.; Whelan, J.; Bosnich, B. *Inorg. Chem.*, preceding paper in this issue.

(2) Schrock, R. R.; Osborn, J. A. *J. Am. Chem. Soc.* **1971**, *93*, 3089.

(3) Schrock, R. R.; Osborn, J. A. *J. Am. Chem. Soc.* **1976**, *98*, 2143.

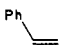
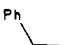
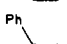
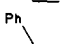
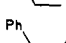
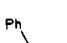
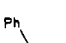
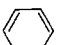
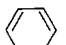
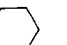
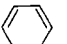
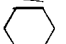
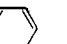
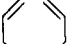
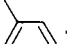
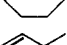
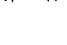
(4) Schrock, R. R.; Osborn, J. A. *J. Am. Chem. Soc.* **1976**, *98*, 4450.

(5) Crabtree, R. H.; Felkin, H.; Morris, G. E. *J. Organomet. Chem.* **1977**, *141*, 205.

(6) Green, M.; Kuc, T. A. *J. Chem. Soc., Dalton Trans.* **1972**, 832.

(7) Crabtree, R. H.; Felkin, H.; Khan, T. F.; Morris, G. E. *J. Organomet. Chem.* **1979**, *168*, 183.

Table I. Homogeneous Hydrogenation of Selected Substrates Employing the Bimetallic Catalyst Precursors $[M_2(\text{diene})_2\text{PNNP}]^{\text{a}}$

substrate	catalyst ^b	products	comments
	Rh		rapid
	Ir		rapid
$\text{Ph}-\text{C}\equiv\text{C}-\text{Ph}$	Rh or Ir	 75%  12%  12%	slow ^c
	Rh	 50%  50%	rapid disprprtation to 1:1 $\text{C}_6\text{H}_6 + \text{C}_6\text{H}_{10}$ followed by slower redn of $\text{C}_6\text{H}_{10} \rightarrow \text{C}_6\text{H}_{12}$
	Ir	  trace	stepwise redn $\text{C}_6\text{H}_8 \rightarrow \text{C}_6\text{H}_{10} \rightarrow \text{C}_6\text{H}_{12}$
 + 	Rh or Ir		no reaction
 + 			

^a Reaction conditions: substrate/catalyst = 150:1, room temperature, 1 atm, CD_3OD . ^b Rh \equiv $[\text{Rh}_2(\text{NBD})_2\text{PNNP}]\text{BF}_4^-$; Ir \equiv $[\text{Ir}_2(\text{COD})_2\text{PNNP}]\text{BF}_4^- \cdot \text{CH}_3\text{OH}$. ^c Product ratios determined by GC.

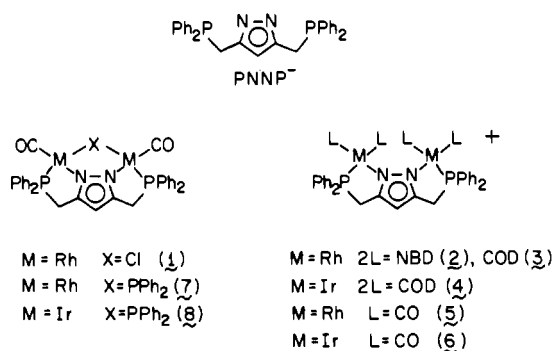


Figure 1. Structures of the ligand PNNP⁻ and of the various homobimetallic complexes derived from it.

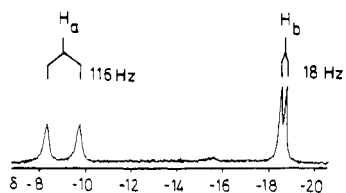


Figure 2. ¹H NMR spectrum of the reaction of $[\text{Ir}_2(\text{COD})_2\text{PNNP}]\text{BF}_4^- + \text{H}_2$ in CD_3OD solution at -78°C . Only the metal hydride region is shown.

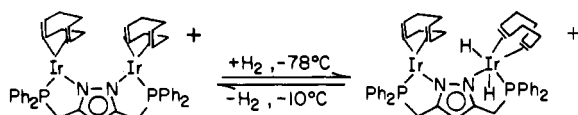


Figure 3. Oxidative addition and reductive elimination of hydrogen with the $[\text{Ir}_2(\text{COD})_2\text{PNNP}]\text{BF}_4^-$ complex in CD_3OD solution. The structure of the dihydride complex was determined by ¹H NMR.

datively adds and reductively eliminates many times before hydrogen transfer to the olefin occurs. At -75°C the dihydride is quite stable and does not reduce the COD within 1 h. It thus appears that the hydrogenation proceeds via one metal at a time and that after the first H_2 has added to one metal, the other metal is deactivated to H_2 addition. This deactivation has been a recurring theme of our studies of these bimetallic systems and is clearly illustrated in other oxidative additions that we now describe.

2. Oxidative-Addition Reactions. Oxidative addition and reductive elimination⁷⁻¹⁰ are fundamental steps in many catalytic

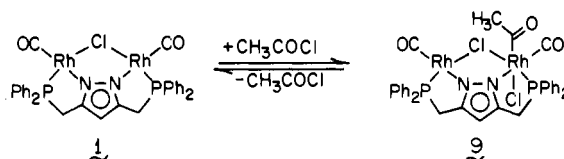


Figure 4. Reversible oxidative addition of acetyl chloride on 1.

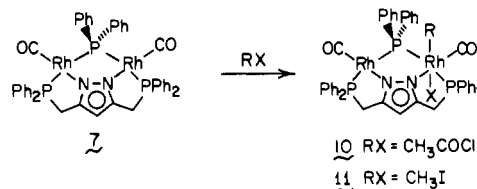


Figure 5. Irreversible oxidative addition of acetyl chloride or methyl iodide on 7.

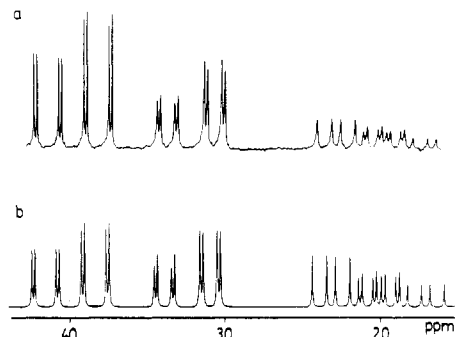
cycles, and if bimetallic complexes were to be used in catalysis, a knowledge of their oxidative-addition-reductive-elimination behavior is an important prerequisite in designing such systems for catalysis. We have just described the reversible exchange of hydrogen with the irridium complex. We now turn to the behavior of these bimetallic complexes with a number of classic electrophiles.

Treatment of the chloro-bridged dirhodium carbonyl complex 1 with acetyl chloride results in a reversible oxidative-addition reaction on one of the metals (Figure 4). The product of this reaction, 9, is best formulated as a Rh(I)-Rh(III) complex on the basis of the following spectroscopic evidence. First, the IR spectrum of 9 displays two bands in the terminal carbonyl region as well as an acyl band. Of the two carbonyl bands ($2107, 1997\text{ cm}^{-1}$), one of these is virtually at the same energy as that observed in 1 (1992 cm^{-1}) and the other is of much higher energy consistent with a higher oxidation state of the metal. Similarly, each of the two inequivalent phosphorus atoms is characterized by very different values for $^1J_{\text{Rh-P}}$ for their ³¹P NMR spectrum. It has been found empirically¹¹ and calculated theoretically¹² that the

- (8) Vaska, L. *Acc. Chem. Res.* **1968**, *1*, 335. Collman, J. P.; Roper, W. R. *Adv. Organomet. Chem.* **1968**, *7*, 53. Lappert, M. F.; Lednor, P. W. *Adv. Organomet. Chem.* **1976**, *14*, 345.
 (9) Yoneda, G.; Blake, D. M. *Inorg. Chem.* **1981**, *20*, 67.
 (10) Crabtree, R. H.; Morehouse, S. M. *Inorg. Chem.* **1982**, *21*, 4210. Louw, W. J.; de Waal, D. J. A.; Gerber, T. I. A.; Demanet, C. M.; Copperthwaite, R. G. *Inorg. Chem.* **1982**, *21*, 1667.
 (11) Meek, D. W.; Mazanec, T. J. *Acc. Chem. Res.* **1981**, *14*, 266.

Table II. IR Data

complex	oxidn state	ν_{CO} , cm^{-1}	$\nu(\text{COCH}_3)$, cm^{-1}
$[\text{Rh}_2(\mu\text{-Cl})(\text{CO})_2\text{PNNP}]$ (1)	I, I	1992	
$[\text{Rh}_2(\mu\text{-PPh}_2)(\text{CO})_2\text{PNNP}]$ (7)	I, I	1956, 1943	
$[\text{Ir}_2(\mu\text{-PPh}_2)(\text{CO})_2\text{PNNP}]$ (8)	I, I	1946, 1926	
$[\text{Rh}_2(\mu\text{-Cl})(\text{CO})_2\text{PNNP}(\text{CH}_3\text{CO})\text{Cl}]$ (9)	I, III	2107, 1997	1695
$[\text{Rh}_2(\mu\text{-PPh}_2)(\text{CO})_2\text{PNNP}(\text{CH}_3\text{CO})\text{Cl}]$ (10)	I, III	2057, 1963	1675
$[\text{Rh}_2(\mu\text{-PPh}_2)(\text{CO})_2\text{PNNP}(\text{CH}_3)\text{I}]$ (11)	I, III	2036, 1978	
$[\text{Ir}_2(\mu\text{-PPh}_2)(\text{CO})_2\text{PNNP}(\text{CH}_3\text{CO})\text{Cl}]$ (13)	I, III	2040, 1959	1648
$[\text{Ir}_2(\mu\text{-PPh}_2)(\text{CO})_2\text{PNNP}(\text{CH}_3)\text{I}]$ (15)	I, III	2020, 1969	
$[\text{Rh}_2(\mu\text{-PPh}_2)(\text{CO})_2\text{PNNP}(\text{CH}_3\text{CO})_2\text{Cl}_2]$ (12)	III, III	2062	1685
$[\text{Ir}_2(\mu\text{-PPh}_2)(\text{CO})_2\text{PNNP}(\text{CH}_3\text{CO})_2\text{Cl}_2]$ (14)	III, III	2048	1650
$[\text{Ir}_2(\mu\text{-PPh}_2)(\text{CO})_2\text{PNNP}(\text{CH}_3)_2\text{I}_2]$ (16)	III, III	2012	

Figure 6. Observed (a) and calculated (b) $^{31}\text{P}\{^1\text{H}\}$ NMR spectrum of 10.

magnitude of $^1J_{\text{Rh-P}}$ is approximately 50% larger for complexes with a formal oxidation state of I than for those with an oxidation state of III. For complex 9, the observed values of $^1J_{\text{Rh-P}}$ of 186 and 135 Hz are in accord with the Rh(I)-Rh(III) formulation of 9.

Replacement of the bridging chloro group in 1 by a diphenylphosphido bridge, 7, results in a significant increase in electron density on each of the metals as evidenced by the reduction of ν_{CO} of 45 cm^{-1} in 7 compared with 1. This enhanced electron richness is manifested in the now *irreversible* oxidative addition of 1 equiv of either acetyl chloride or methyl iodide to 7 (Figure 5). Again, the products of these reactions, 10 and 11, are best formulated as Rh(I)-Rh(III) complexes on the basis of their IR and, particularly, their ^{31}P NMR spectra. The ^{31}P NMR spectra are complicated by the presence of five inequivalent, magnetically active nuclei. The ^{31}P NMR spectrum of 10 and a computer simulation are shown in Figure 6. There are four different $^1J_{\text{Rh-P}}$ coupling constants, two of which (128 and 122 Hz) are approximately 50% larger than the other two (89 and 75 Hz) as would be expected for the Rh(I)-Rh(III) formulation. Perhaps surprisingly there is a small coupling observed between the two phosphorus atoms of PNNP ($^4J_{\text{P-P}} = 11\text{ Hz}$). The chemical shift of the phosphido bridge phosphorus atom is consistent with the absence of a metal-metal bond.¹³ This is supported by the crystal structure of 11 that we describe later.

The increased electron richness of the metals in the phosphido-bridged species compared to the chloro-bridged analogue is evidenced by the ability of both metals to add electrophilic substrates. Treatment of the monoacyl complex, 10, with acetyl chloride results in the *reversible* formation of the corresponding diacyl complex, 12 (Figure 7). Despite the large number of potential isomers possible for 12, the IR and ^1H and ^{31}P NMR spectra suggest a high degree of symmetry; one ^1H NMR methyl signal and one acyl CO and one CO band (IR) are observed. The equilibrium constant for the addition of the second acetyl chloride is found to be 2.7 ± 0.5 by ^1H NMR in CDCl_3 solution at 30°C .

The corresponding phosphido-bridged iridium complexes appear to be much more effective in oxidative addition as expected. With the iridium complexes, two successive, *irreversible* oxidative additions occur with either acetyl chloride or methyl iodide to give

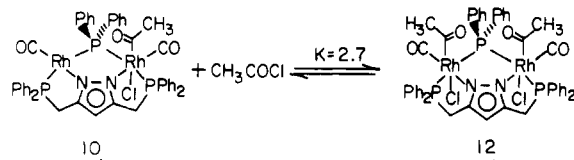
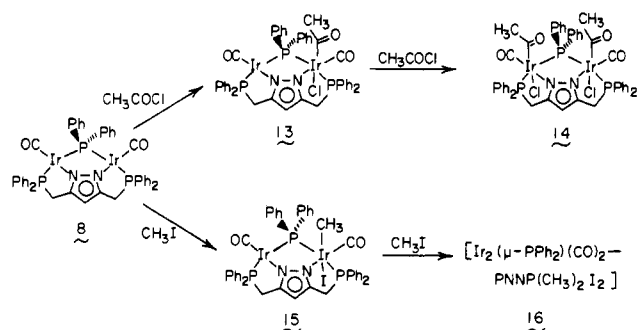
Figure 7. Reversible acetyl chloride oxidative addition on 10. The ^1H NMR shows that the methyl groups are magnetically equivalent in 12 but the isomerism is not known.

Figure 8. Various oxidative additions of 8.

the diacyl, 14, and dimethyl, 16, complexes, respectively (Figure 8). The intermediate monoacyl, 13, and monomethyl, 15, species can be isolated but with difficulty because of their susceptibility to the succeeding oxidative addition. Spectroscopically, the monoacyl, diacyl, and monomethyl complexes appear to exist as one isomer. The dimethyl complex, 16, however, is a mixture of geometric isomers ($\sim 1:2:3$), giving three separate ^1H NMR methyl signals and three sets of signals in the ^{31}P NMR spectrum. Within each isomer the two methyl groups appear to be magnetically equivalent. There are four possible isomers that fit these requirements, but we have not found it possible to assign the isomers.

The bimetallic complexes display four types of oxidative-addition behavior, namely: reversible $\text{M(I)-M(I)} \rightleftharpoons \text{M(I)-M(III)}$, irreversible $\text{M(I)-M(I)} \rightarrow \text{M(I)-M(III)}$, reversible $\text{M(I)-M(III)} \rightleftharpoons \text{M(III)-M(III)}$, and irreversible $\text{M(I)-M(III)} \rightarrow \text{M(III)-M(III)}$ oxidation state changes. This behavior may be correlated with the electron richness of the metals: the more electron rich the metals, the greater the tendency to oxidatively add irreversibly to give the III oxidation state. The IR data for these complexes (Table II) are consistent with this assumption. First, for the three M(I)-M(I) complexes, ν_{CO} decreases in the order $1 > 7 > 8$ which reflects the increasing drive to oxidative addition. The same trend is seen for the three monoacyl complexes, 9, 10 and 13, for which both the ν_{CO} and ν_{COCH_3} vary in the expected order ($9 > 10 > 13$). It therefore appears that the predominant factor that determines the extent of oxidative addition is an electronic effect. The IR data may also be used to explain the apparent deactivation of the second metal to reaction after the first has undergone oxidative addition. Thus, considering the ν_{CO} for 8, 13 and 15, the frequencies suggest a decrease in electron richness for the Ir(I) center after the other iridium center has undergone oxidative addition. There may of course be steric factors that lower the tendency to oxidative addition, but taken as a whole, the data indicate that

(12) Nixon, J. F.; Pidcock, A. *Ann. Rev. NMR Spectrosc.* 1969, 2, 345.(13) Petersen, J. L.; Stewart, R. P. *Inorg. Chem.* 1980, 19, 186.

Table III. Selected Distances (Å) and Angles (deg) for **11** with Standard Deviations in Parentheses^a

Distances		Angles			
(a) About Rhodium(1)					
Rh(1)–I	2.8042 (4)	C(12)–Rh(1)–C(11)	93.1 (2)	P(2)–Rh(1)–I	85.13 (3)
Rh(1)–C(12)	2.295 (6)	C(12)–Rh(1)–P(2)	93.4 (1)	P(2)–Rh(1)–N(1)	78.52 (9)
Rh(1)–P(1)	2.395 (1)	C(12)–Rh(1)–N(1)	87.8 (1)	I–Rh(1)–N(1)	89.56 (8)
Rh(1)–P(2)	2.375 (1)	C(12)–Rh(1)–P(1)	82.1 (1)	I–Rh(1)–P(1)	98.79 (3)
Rh(1)–N(1)	2.058 (3)	C(11)–Rh(1)–P(2)	99.0 (1)	N(1)–Rh(1)–P(1)	86.71 (9)
Rh(1)–C(11)	1.845 (4)	C(11)–Rh(1)–I	89.6 (1)	C(12)–Rh(1)–I	177.14 (9)
		C(11)–Rh(1)–P(1)	95.8 (1)	C(11)–Rh(1)–N(1)	177.4 (2)
Rh(1)···Rh(2)	3.766			P(1)–Rh(1)–P(2)	164.72 (3)
C(11)–O(11)	1.129 (5)			Rh(1)–C(11)–O(11)	178.1 (4)
(b) About Rhodium(2)					
Rh(2)–P(1)	2.369 (1)	P(1)–Rh(2)–C(21)	96.3 (1)	P(1)–Rh(2)–N(2)	87.30 (8)
Rh(2)–P(3)	2.302 (1)	P(3)–Rh(2)–C(21)	97.0 (1)	P(1)–Rh(2)–P(3)	166.66 (4)
Rh(2)–N(2)	2.033 (3)	P(3)–Rh(2)–N(2)	79.38 (8)	N(2)–Rh(2)–C(21)	176.1 (2)
Rh(2)–C(21)	1.809 (5)				
C(21)–O(21)	1.126 (5)	Rh(1)–P(1)–Rh(2)	104.47 (4)	Rh(2)–C(21)–O(21)	177.9 (5)

^a Bond distances and bond angles in the PNNP ligand have been deposited as supplementary material.

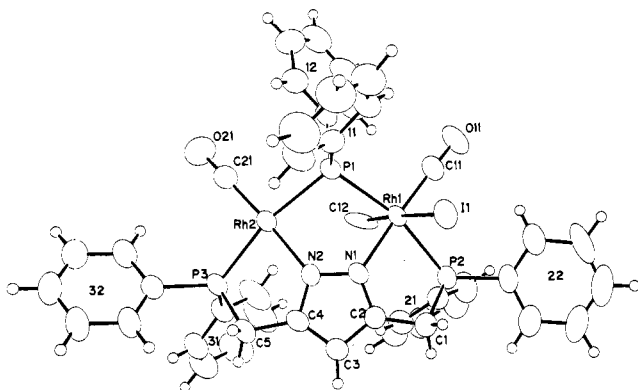


Figure 9. ORTEP view of the molecule $[\text{Rh}_2(\mu\text{-PPH}_2)(\text{CO})_2\text{PNNP}(\text{CH}_3)\text{I}]$. Thermal ellipsoids are drawn at the 50% probability level.

these factors are not crucial for the electrophiles we have used. It appears therefore that after the first addition there is electronic transmission via the bridges so that charge is transferred from the M(I) to the M(III) center. Presumably if the PNNP were not constraining the two metals, this electronic charge transfer could lead to the metal–metal bond formation.

3. Crystal Structure of $[\text{Rh}_2(\mu\text{-PPH}_2)(\text{CO})_2\text{PNNP}(\text{CH}_3)\text{I}]\cdot\text{C}_6\text{H}_{10}\text{O}$ (11**).** The structure of $[\text{Rh}_2(\mu\text{-PPH}_2)(\text{CO})_2\text{PNNP}(\text{CH}_3)\text{I}]$ and the atomic numbering scheme are shown in Figure 9. Selected bond distances and angles are collected in Table III. The molecule has two rhodium atoms in the formal oxidation states of I and III, and the lattice also contains diethyl ether molecules.

The geometry about Rh(1) is approximately octahedral, with the methyl and iodo ligands in trans positions. Distortions from octahedral geometry arise from the inability of the P(2)–N(1) chelate to achieve a 90° “bite angle” (P(2)–Rh(1)–N(1) = 78.52 (9)°) which results in a P(1)–Rh(1)–P(2) angle of 164.72 (3)°. In the I oxidation state, rhodium Rh(2) is approximately square planar with P(1)–Rh(2)–P(3) and N(2)–Rh(2)–C(21) angles of 166.66 (4) and 176.1 (2)°, respectively. Again, these angles appear to reflect the small bite angle of the N(2)–P(3) chelate (79.38 (8)°). These small bite angles are comparable to those observed in other five-membered chelate rings in bis(phosphine)- or diminerhodium complexes^{14,15} (79–83°).

The metal–ligand distances are within the range normally observed,¹⁶ and they are correspondingly uniformly shorter for

the four-coordinate rhodium(I) than for the six-coordinate rhodium(III) center. This has been observed before¹⁷ and may reflect the stronger π bonding of the rhodium(I) center to the π -acid ligands. The rhodium–methyl bond appears to be significantly longer (2.295 (6) Å) than the few other known rhodium(III)–carbon distances (2.090 (4),¹⁴ 2.130 (28),¹⁸ 2.26 Å¹⁹).

The long Rh(1)–Rh(2) separation (3.766 Å) corresponds to the absence of a metal–metal bond and may be compared with other rhodium structures without metal–metal bonds (3.3–3.8 Å)^{18,20,21} and with those that do possess metal–metal bonds (2.7–2.8 Å).^{22,23} The large Rh(1)–P(1)–Rh(2) angle (104.47 (4)°) is also consistent with absence of a metal–metal bond.²⁴

Bond distances and angles in the PNNP ligand are normal and comparable to those found for $[\text{Rh}_2(\mu\text{-3,5-dimethylpyrazole})_2(\text{PPh}_2)_2(\text{CS})_2]$.²⁵ The pyrazole ring of PNNP is planar to ± 0.017 (5) Å with the phosphorus atoms P(2) and P(3) well above and the phosphido phosphorus atom P(1) well below this plane (Table V). As a result an overall fold is imparted to the molecule so that the mean molecular planes encompassing the two metals form an angle of 146.3°.

4. Discussion. The object of this work, to design a bimetallic system that was incapable of metal–metal bond formation but where the metals were held rigidly within cooperative distances, appears to have been realized with the PNNP ligand. We have concentrated on oxidative-addition and reductive-elimination

(14) Collman, J. P.; Cristian, P. A.; Current, S.; Denisevich, P.; Halbert, T. R.; Schmittou, E. R.; Hodgson, K. O. *Inorg. Chem.* **1976**, *15*, 223.
 (15) Hall, M. C.; Kilbourn, B. T.; Taylor, K. A. *J. Chem. Soc. A* **1970**, 2539.

(16) Rh(I)–N and Rh(I)–CO: Uson, R.; Oro, L. A.; Cirano, M. A.; Pinillos, M. T.; Tiripicchio, A.; Camellini, M. T. *J. Organomet. Chem.* **1981**, *205*, 247. Rh(I)–P: Wajda, K.; Pruchnick, F.; Lis, T. *Inorg. Chim. Acta* **1980**, *40*, 207. Rh(I)–P: Meek, D. W.; Kreter, P. E.; Christoph, G. G. *J. Organomet. Chem.* **1982**, *231*, C53. Rh(III)–N: Roziere, J.; Lehmann, M. S.; Potier, J. *Acta Crystallogr., Sect. B: Struct. Crystallogr. Cryst. Chem.* **1979**, *B35*, 1099. Rh(III)–Co: Doyle, M. J.; Mayanza, A.; Bonnet, J. J.; Kalck, P.; Poilblanc, R. *J. Organomet. Chem.* **1978**, *146*, 293. Rh(III)–P: McGinney, J. A.; Payne, N. C.; Ibers, J. A. *J. Am. Chem. Soc.* **1969**, *91*, 6301. Rh(III)–I: reference 14. Hitchcock, P. B.; Lappert, M. F.; McLaughlin, G. M.; Oliver, A. J. *J. Chem. Soc., Dalton Trans.* **1974**, 68.
 (17) Meier, E. B.; Burch, R. R.; Muettterties, E. L.; Day, V. W. *J. Am. Chem. Soc.* **1982**, *104*, 2661.
 (18) Doyle, M. J.; Mayanza, A.; Bonnet, J. J.; Kalck, P.; Poilblanc, R. *J. Organomet. Chem.* **1978**, *146*, 293.
 (19) Paulus, E. F.; Fritz, H. P.; Schwarzhaus, K. E. *J. Organomet. Chem.* **1968**, *11*, 647.
 (20) Cowie, M.; Southern, T. G. *Inorg. Chem.* **1982**, *21*, 246.
 (21) Uson, R.; Oro, L. A.; Cirano, M. A.; Pinillos, M. T.; Tiripicchio, A.; Camellini, M. T. *J. Organomet. Chem.* **1981**, *205*, 247.
 (22) Meek, D. W.; Kreter, P. E.; Christoph, G. G. *J. Organomet. Chem.* **1982**, *231*, C53.
 (23) Kubiak, C. P.; Woodcock, C.; Eisenberg, R. *Inorg. Chem.* **1982**, *21*, 2119.
 (24) Dahl, L. F.; de Gil, E. R.; Feltham, R. D. *J. Am. Chem. Soc.* **1969**, *91*, 1653.
 (25) Uson, R.; Oro, L. A.; Cirano, M. A.; Carmona, D.; Tiripicchio, A.; Camellini, M. T. *J. Organomet. Chem.* **1982**, *224*, 69.

Table IV. Positional Parameters and Their Estimated Standard Deviations

atom	x	y	z	B ^a , Å ²
I(1)	0.07342 (3)	0.11216 (3)	0.23438 (3)	4.078 (8)
Rh(1)	0.24739 (3)	0.25241 (3)	0.15800 (3)	2.798 (8)
Rh(2)	0.27742 (3)	0.40770 (3)	0.32765 (3)	3.132 (8)
P(1)	0.3187 (1)	0.2425 (1)	0.28664 (9)	3.06 (3)
P(2)	0.1540 (1)	0.3040 (1)	0.04251 (9)	3.30 (3)
P(3)	0.2046 (1)	0.5698 (1)	0.35080 (9)	3.44 (3)
O(11)	0.4024 (4)	0.0865 (3)	0.0772 (3)	5.9 (1)
O(21)	0.4687 (4)	0.4068 (4)	0.4054 (4)	7.9 (1)
N(1)	0.1344 (3)	0.3666 (3)	0.2093 (3)	3.03 (9)
N(2)	0.1450 (3)	0.4208 (3)	0.2719 (3)	3.03 (9)
C(1)	0.0196 (5)	0.3636 (4)	0.1076 (4)	3.7 (1)
C(2)	0.0457 (4)	0.4077 (4)	0.1793 (3)	3.3 (1)
C(3)	-0.0038 (4)	0.4904 (4)	0.2230 (4)	3.5 (1)
C(4)	0.0610 (4)	0.4952 (4)	0.2803 (3)	3.3 (1)
C(5)	0.0561 (5)	0.5644 (4)	0.3471 (4)	3.8 (1)
C(11)	0.3450 (5)	0.1499 (4)	0.1084 (4)	3.9 (1)
C(12)	0.3828 (6)	0.3736 (5)	0.0959 (4)	5.4 (1)
C(21)	0.3949 (5)	0.4054 (5)	0.3764 (4)	4.7 (1)
O(4)	0.3742 (8)	0.2383 (7)	0.6908 (6)	14.3 (3)*
C(6)	0.329 (2)	0.247 (1)	0.621 (1)	18.3 (6)*
C(7)	0.245 (1)	0.333 (1)	0.630 (1)	14.1 (5)*
C(8)	0.471 (2)	0.155 (1)	0.680 (1)	18.0 (6)*
C(9)	0.461 (2)	0.125 (1)	0.766 (1)	17.1 (6)*
C(111)	0.2490 (5)	0.1445 (4)	0.3799 (4)	3.6 (1)
C(112)	0.1739 (6)	0.1714 (5)	0.4596 (4)	5.0 (2)
C(113)	0.1220 (8)	0.0947 (7)	0.5295 (5)	7.5 (2)
C(114)	0.1425 (7)	-0.0054 (6)	0.5211 (5)	6.6 (2)
C(115)	0.2179 (7)	-0.0328 (5)	0.4450 (5)	6.1 (2)
C(116)	0.2691 (6)	0.0397 (4)	0.3740 (4)	4.8 (2)
C(121)	0.4693 (4)	0.1944 (4)	0.2714 (4)	3.6 (1)
C(122)	0.5515 (5)	0.1887 (4)	0.1866 (5)	4.6 (1)
C(123)	0.6633 (5)	0.1547 (5)	0.1805 (5)	5.7 (2)
C(124)	0.6976 (5)	0.1252 (6)	0.2545 (6)	6.4 (2)
C(125)	0.6202 (6)	0.1287 (6)	0.3409 (5)	6.9 (2)
C(126)	0.5063 (5)	0.1641 (5)	0.3482 (5)	5.2 (2)
C(211)	0.2225 (5)	0.4072 (4)	-0.0478 (4)	3.6 (1)
C(212)	0.2852 (7)	0.3878 (5)	-0.1311 (4)	5.6 (2)
C(213)	0.3415 (8)	0.4660 (7)	-0.1953 (5)	7.4 (2)
C(214)	0.3341 (7)	0.5627 (5)	-0.1769 (5)	6.5 (2)
C(215)	0.2738 (6)	0.5824 (5)	-0.0938 (5)	5.4 (2)
C(216)	0.2166 (6)	0.5065 (5)	-0.0293 (4)	4.6 (1)
C(221)	0.1082 (5)	0.2222 (4)	-0.0195 (4)	4.0 (1)
C(222)	0.0253 (7)	0.2603 (6)	-0.0630 (5)	6.5 (2)
C(223)	-0.0095 (7)	0.2018 (7)	-0.1136 (5)	8.3 (2)
C(224)	0.0379 (8)	0.1086 (7)	-0.1235 (5)	8.5 (2)
C(225)	0.1172 (9)	0.0670 (6)	-0.0798 (6)	9.1 (3)
C(226)	0.1564 (7)	0.1259 (6)	-0.0284 (5)	6.8 (2)
C(311)	0.2594 (5)	0.6715 (4)	0.2562 (4)	4.0 (1)
C(312)	0.2245 (6)	0.7723 (4)	0.2606 (4)	4.8 (1)
C(313)	0.2619 (7)	0.8483 (5)	0.1845 (5)	6.3 (2)
C(314)	0.3313 (8)	0.8216 (6)	0.1038 (6)	7.7 (2)
C(315)	0.3658 (9)	0.7224 (6)	0.1005 (6)	8.6 (3)
C(316)	0.3296 (7)	0.6464 (5)	0.1755 (5)	6.7 (2)
C(321)	0.1938 (5)	0.6256 (4)	0.4514 (4)	3.8 (1)
C(322)	0.0924 (5)	0.6643 (4)	0.5027 (4)	4.5 (1)
C(323)	0.0860 (6)	0.7054 (5)	0.5791 (4)	4.9 (1)
C(324)	0.1833 (7)	0.7078 (5)	0.6043 (4)	5.9 (2)
C(325)	0.2856 (6)	0.6712 (7)	0.5523 (5)	8.9 (2)
C(326)	0.2911 (6)	0.6295 (6)	0.4765 (5)	7.3 (2)

^a Starred values refer to atoms refined isotropically. Anisotropically refined atoms are given in the form of the isotropic equivalent thermal parameter defined as $\frac{1}{3}[a^2B(1,1) + b^2B(2,2) + c^2B(3,3) + ab(\cos \gamma)B(1,2) + ac(\cos \beta)B(1,3) + bc(\cos \alpha)B(2,3)]$.

reactions of our bimetallic rhodium and iridium complexes. A recurring observation in these studies is that oxidative addition at one center leads to deactivation (toward oxidative addition) at the other. The dominant source of deactivation appears to be electronic in that the lower oxidation state metal transfers some of its electron charge to the higher oxidation state metal via the bridging ligands. We suspect that this may be a general phenomenon with multimetallic systems and, in the absence of restraining bridges or other ligands, leads to metal-metal bond formation after the first metal has undergone oxidative addition.

Table V. Least-Squares Mean Planes and Deviations (Å) of Other Atoms from These Planes

(1) Atoms Defining Plane: N(1), N(2), C(1), C(2), C(3), C(4), C(5)			
Eq of Plane: $0.4798x + 0.5053y - 0.7173z = 1.9985$			
P(1)	-0.384 (1)	C(111)	-2.170 (5)
P(2)	0.829 (1)	C(121)	0.254 (5)
P(3)	0.890 (1)	C(211)	2.625 (5)
Rh(1)	0.181 (1)	C(221)	0.400 (6)
Rh(2)	0.293 (1)	C(311)	2.624 (6)
C(11)	0.353 (6)	C(321)	0.523 (5)
C(21)	0.619 (6)		
(2) Atoms Defining Plane: Rh(1), P(1), P(2), C(11), N(1)			
Eq of Plane: $0.6260x + 0.5990y - 0.4993z = 3.6598$			
Rh(1)	-0.028 (1)	N(1)	-0.044 (4)
P(1)	0.050 (1)	C(1)	-0.646 (6)
P(2)	0.053 (1)	C(2)	-0.273 (5)
C(11)	-0.032 (6)	O(11)	-0.055 (5)
(3) Atoms Defining Plane: Rh(1), C(11), C(12), N(1), I			
Eq of Plane: $-0.5523x + 0.0729y - 0.8305z = -3.888$			
Rh(1)	-0.026 (1)	N(1)	0.014 (4)
C(11)	0.016 (6)	I	-0.002 (1)
C(12)	-0.003 (6)	O(11)	0.069 (5)
(4) Atoms Defining Plane: Rh(2), P(1), P(3), N(2), C(21)			
Eq of Plane: $0.3853x + 0.2440y - 0.8899z = -0.6605$			
Rh(2)	-0.015 (1)	C(21)	0.008 (6)
P(1)	0.001 (1)	C(4)	-0.201 (5)
P(3)	0.000 (1)	C(5)	-0.679 (5)
N(2)	0.007 (4)	O(21)	0.050 (5)

dihedral angle between planes 2 and 4: 146.3°

dihedral angle between planes 2 and 3: 83.5°

The mutual interaction that occurs for the PNNP system allows for the tuning of the system for either single or double oxidative addition. Thus, we have observed a spectrum of reactivity from a single reversible oxidative addition to irreversible double oxidative addition. This was achieved by adjusting the electron density on the two metals. This mutual deactivation may be advantageous in the sense that the metal that is deactivated to oxidative addition appears to be activated to reductive elimination. Thus, it may be possible to induce reductive elimination in one metal by oxidative addition to the other. It is conceivable that such a phenomenon could be exploited in catalysis although, as we have seen for hydrogenation, the two metals appears to react independently.

Many of the unique reactivity patterns associated with "A-frame" molecules,^{20,23,26} some phosphido-bridged systems,²⁷ and, to a lesser degree, the bis(pyrazole)²⁸ bimetallics are derived from the fact that the ligands are sufficiently flexible to allow for a spectrum of metal-metal interactions. The present work therefore serves to illustrate how the absence of direct metal-metal interaction gives rise to different reactivity patterns.

Experimental Section

All reactions using rhodium(I) or iridium(I) complexes were performed under N₂ or Ar by using standard Schlenk techniques. The preparation of complexes 1-8 is described elsewhere.¹ ¹H NMR spectra, recorded on Varian T-60 or XL-200 spectrometers, are reported for CDCl₃ solutions relative to Me₄Si unless stated otherwise. ³¹P NMR spectra were recorded on Bruker WP-80 or Varian XL-200 spectrometers

- (26) Lee, C. L.; Hunt, C. T.; Balch, A. L. *Inorg. Chem.* **1981**, *20*, 2498. Fischer, J. R.; Mills, A. J.; Sumner, S.; Brown, M. P.; Thomson, M. A.; Puddephatt, R. J.; Frew, A. A.; Manojlovic-Muir, L.; Muir, K. W. *Organometallics* **1982**, *1*, 1421 and references cited therein.
- (27) Collman, J. P.; Rothrock, R. K.; Finke, R. G.; Moore, E. J.; Rose-Munch, F. *Inorg. Chem.* **1982**, *21*, 146. Yu, Y. F.; Gallucci, J.; Wojcicki, A. J. *Am. Chem. Soc.* **1983**, *105*, 4826. Breen, M. J.; Geoffroy, G. L.; Rheingold, A. L.; Fultz, W. C. *J. Am. Chem. Soc.* **1983**, *105*, 1069. Breen, M. J.; Duttera, M. R.; Geoffroy, G. L.; Novotnak, G. C.; Roberts, D. A.; Shulman, P. M.; Steinmetz, G. R. *Organometallics* **1982**, *1*, 1008.
- (28) Beveridge, K. A.; Bushnell, G. W.; Dixon, K. R.; Eadie, D. T.; Stobart, S. R.; Atwood, J. L.; Zaworotko, M. J. *J. Am. Chem. Soc.* **1982**, *104*, 920. Coleman, A. W.; Eadie, D. T.; Stobart, S. R.; Zaworotko, M. J.; Atwood, J. L. *J. Am. Chem. Soc.* **1982**, *104*, 922.

Table VI. ^{31}P NMR Data^a

	δ_{Pb}	δ_{P1}	δ_{P2}	$^2J_{\text{P1-Pb}}$	$^2J_{\text{P2-Pb}}$	$^4J_{\text{P1-P2}}$	$^1J_{\text{M1-P1}}$	$^1J_{\text{M1-Pb}}$	$^1J_{\text{M2-P2}}$	$^1J_{\text{M2-Pb}}$
	$\text{M}^{\text{I}}\text{M}^{\text{IIIb}}$									
$[\text{Rh}_2(\mu\text{-Cl})(\text{CO})_2\text{PNNP}(\text{CH}_3\text{CO})\text{Cl}]$		58.33	53.17				186		135	
$[\text{Rh}_2(\mu\text{-PPh}_2)(\text{CO})_2\text{PNNP}(\text{CH}_3\text{CO})\text{Cl}]$	21.42	40.70	33.16	263	240	11	128	122	89	75
$[\text{Ir}_2(\mu\text{-PPh}_2)(\text{CO})_2\text{PNNP}(\text{CH}_3\text{CO})\text{Cl}]$	-11.48	35.84	15.08	257	224	8				
$[\text{Ir}_2(\mu\text{-PPh}_2)(\text{CO})_2\text{PNNP}(\text{CH}_3)\text{I}]$	-12.71	34.70	13.32	253	264	9				
	$\text{M}^{\text{III}}\text{M}^{\text{III}}$									
$[\text{Ir}_2(\mu\text{-PPh}_2)(\text{CO})_2\text{PNNP}(\text{CH}_3\text{CO})_2\text{Cl}_2]$	-42.27	8.86		254						
$[\text{Ir}_2(\mu\text{-PPh}_2)(\text{CO})_2\text{PNNP}(\text{CH}_3)_2\text{I}_2]$										
isomer A	-52.92	27.31	27.30	288	276					
isomer B	-18.36	2.81	2.74	310	261					
isomer C	-21.88	10.80	10.78	298	267					

^aRecord of CHCl_3 or CH_2Cl_2 solutions on a Varian XL-200 (80.96 MHz); J values in Hz. ^bSpin system defined as $\text{P}_1\text{-M}^{\text{I}}\text{-P}_b\text{-M}^{\text{III}}\text{-P}_2$. The larger value of $^1J_{\text{Rh-P}}$ is assigned to Rh^I. Where ambiguity exists (Ir), P₁ is assigned as farthest downfield.

(operating at 32.3 or 80.96 MHz, respectively) for CH_2Cl_2 solutions with a coaxial 4-mm sealed glass insert containing $\text{C}_6\text{D}_6/\text{P}(\text{OMe})_3$ (lock/reference), and chemical shifts are reported relative to 85% H_3PO_4 . Infrared spectra were recorded on a Perkin-Elmer 337 spectrometer on solid samples (Nujol mull). The ^{31}P NMR spectra for all new compounds are collected in Table VI and the IR data in Table II.

Catalytic Hydrogenation Monitored by ^1H NMR. The homogeneous hydrogenation of the substrates presented in Table I was performed as follows. A solution of the substrate (3.3×10^{-3} mol) and either catalyst ($[\text{Rh}_2(\text{NBD})_2\text{PNNP}]\text{BF}_4$ or $[\text{Ir}_2(\text{COD})_2\text{PNNP}]\text{BF}_4 \cdot \text{CH}_3\text{OH}$) (2.6×10^{-5} mol) in CD_3OD (0.4 mL) in a 5-mm ^1H NMR tube was bubbled with $\text{H}_2(\text{g})$ at atmospheric pressure. The progress of the reaction was monitored periodically.

$[\text{Rh}_2(\mu\text{-Cl})(\text{CO})_2\text{PNNP}(\text{CH}_3\text{CO})\text{Cl}]$ (9). This complex was generated in solution and characterized spectroscopically as follows. A suspension of $[\text{Rh}_2(\mu\text{-Cl})(\text{CO})_2\text{PNNP}]$ in CDCl_3 in an NMR tube was treated with CH_3COCl (2 equiv). The solid dissolved to give a clear yellow solution. ^1H NMR: δ 1.72 (s, 3 H), 3.97 (d, $J = 12.5$ Hz, 2 H), 4.16 (d, $J = 12.5$ Hz, 2 H), 6.26 (s, 1 H), 7.1–8.3 (m, 20 H).

$[\text{Rh}_2(\mu\text{-PPh}_2)(\text{CO})_2\text{PNNP}(\text{CH}_3\text{CO})\text{Cl}]$ (10). To a suspension of $[\text{Rh}_2(\mu\text{-PPh}_2)(\text{CO})_2\text{PNNP}]$ (0.25 g, 0.275 mmol) in CH_2Cl_2 (4 mL) was added CH_3COCl (21 μL , 0.296 mmol). When all of the starting material had dissolved (~ 20 min), ether was added (25 mL in 5-mL portions) to give 0.25 g (93%) of yellow needles. ^1H NMR: δ 1.23 (s, 3 H), 4.1 (m, 4 H), 6.13 (s, 1 H), 7.0–8.5 (m, 30 H). Anal. Calcd for $\text{C}_{45}\text{H}_{38}\text{ClN}_2\text{O}_3\text{P}_3\text{Rh}_2$: C, 54.65; H, 3.87; Cl, 3.58; N, 2.83; P, 9.40. Found: C, 54.68; H, 3.88; Cl, 3.83; N, 2.83; P, 9.67.

$[\text{Rh}_2(\mu\text{-PPh}_2)(\text{CO})_2\text{PNNP}(\text{CH}_3\text{CO})\text{Cl}] \cdot 1.5\text{CH}_2\text{Cl}_2$ (12). This complex was prepared by treatment of either a suspension (CH_2Cl_2) of $[\text{Rh}_2(\mu\text{-PPh}_2)(\text{CO})_2\text{PNNP}(\text{CH}_3\text{CO})\text{Cl}]$ with CH_3COCl (25 equiv) followed by precipitation with ether. ^1H NMR (CD_2Cl_2 , in the presence of excess CH_3COCl): δ 1.33 (s, 6 H), 4.5 (m, 4 H), 6.60 (s, 1 H), 7.0–8.6 (m, 30 H). Anal. Calcd for $\text{C}_{47}\text{H}_{41}\text{Cl}_2\text{N}_2\text{O}_4\text{P}_3\text{Rh}_2 \cdot 1.5\text{CH}_2\text{Cl}_2$: C, 48.75; H, 3.71; Cl, 14.84; N, 2.34; O, 5.36; P, 7.78. Found: C, 49.36; H, 3.76; Cl, 15.38; N, 2.41; O, 5.33; P, 8.13.

Determination of K_{eq} for $10 + \text{CH}_3\text{COCl} \rightleftharpoons 12$. The equilibrium constant was determined by obtaining values for the concentrations of the three species involved by integration of the ^1H NMR spectra (CD_2Cl_2 , 60 MHz) obtained upon successive additions of CH_3COCl to 10 (up to 15 equiv).

$[\text{Rh}_2(\mu\text{-PPh}_2)(\text{CO})_2\text{PNNP}(\text{CH}_3)\text{I}] \cdot \text{C}_4\text{H}_{10}\text{O}$ (11). A suspension of $[\text{Rh}_2(\mu\text{-PPh}_2)(\text{CO})_2\text{PNNP}]$ (0.15 g, 0.165 mmol) in CH_2Cl_2 (2 mL) was treated with CH_3I (11.3 μL , 0.181 mmol) and was stirred until all of the starting material had dissolved (~ 20 min). The addition of ether (30 mL) gave golden yellow blocks, 0.17 g (92%). ^1H NMR: δ 0.45 (m, 3 H), 1.18 (t, $J = 7$ Hz, 6 H), 3.43 (q, $J = 7$ Hz, 4 H), 4.13 (m, 4 H), 6.00 (s, 1 H), 6.8–8.5 (m, 30 H). Anal. Calcd for $\text{C}_{44}\text{H}_{38}\text{IN}_2\text{O}_3\text{P}_3\text{Rh}_2 \cdot \text{C}_4\text{H}_{10}\text{O}$: C, 51.18; H, 4.29; I, 11.26; N, 2.49; P, 8.25. Found: C, 50.88; H, 4.10; I, 11.51; N, 2.56; P, 8.43.

$[\text{Ir}_2(\mu\text{-PPh}_2)(\text{CO})_2\text{PNNP}(\text{CH}_3\text{CO})\text{Cl}]$ (13). A suspension of $[\text{Ir}_2(\mu\text{-PPh}_2)(\text{CO})_2\text{PNNP}]$ (0.35 g, 0.321 mmol) in CH_2Cl_2 (4 mL) was treated with CH_3COCl (25 μL , 0.352 mmol) and was stirred for 15 min during which time all of the solid had dissolved. Yellow needles of the product (0.34 g, 91%) were obtained by the addition of ether (40 mL). In spite of several attempts, this product invariably contained small amounts of the corresponding diacyl complex; however, this did not hinder spectroscopic characterization. ^1H NMR: δ 1.03 (s, 3 H), 4.3 (m, 4 H), 6.20 (s, 1 H), 7.0–8.6 (m, 30 H).

$[\text{Ir}_2(\mu\text{-PPh}_2)(\text{CO})_2\text{PNNP}(\text{CH}_3)\text{I}]$ (15). To a suspension of $[\text{Ir}_2(\mu\text{-PPh}_2)(\text{CO})_2\text{PNNP}]$ (0.285 g, 0.26 mmol) in CH_2Cl_2 (10 mL) was added

CH_3I (17.5 μL , 0.28 mmol). The solution was stirred for 15 min, and then ether (60 mL in portions) was added. The resulting yellow solid (which invariably contained a small amount of the corresponding dimethyl complex) was filtered, washed with ether, and dried; 0.28 g (82%). ^1H NMR: δ 0.07 (t, $J = 5.5$ Hz, 3 H), 4.33 (m, 4 H), 6.17 (s, 1 H), 6.9–8.4 (m, 30 H).

$[\text{Ir}_2(\mu\text{-PPh}_2)(\text{CO})_2\text{PNNP}(\text{CH}_3\text{CO})_2\text{Cl}_2]$ (14). To a suspension of $[\text{Ir}_2(\mu\text{-PPh}_2)(\text{CO})_2\text{PNNP}]$ (0.25 g, 0.23 mmol) in CH_2Cl_2 (5 mL) was added CH_3COCl (36 μL , 0.51 mmol). This resulted in immediate dissolution of the starting material to give a clear, yellow solution that slowly decolorized to a very pale yellow. The solution was stirred for 2 h, and the product was crystallized by the addition of ether (40 mL) to obtain off-white needles, 0.24 g (86%). ^1H NMR: δ 0.87 (s, 6 H), 4.57 (d, $J = 10$ Hz, 4 H), 6.62 (s, 1 H), 7.0–8.5 (m, 30 H). Anal. Calcd for $\text{C}_{47}\text{H}_{41}\text{Cl}_2\text{N}_2\text{O}_4\text{P}_3\text{Ir}_2$: C, 45.30; H, 3.32; Cl, 5.69; N, 2.25; P, 7.46. Found: C, 45.22; H, 3.49; Cl, 5.98; N, 2.29; P, 7.16.

$[\text{Ir}_2(\mu\text{-PPh}_2)(\text{CO})_2\text{PNNP}(\text{CH}_3)_2] \cdot \text{C}_4\text{H}_{10}\text{O}$ (16). A suspension of $[\text{Ir}_2(\mu\text{-PPh}_2)(\text{CO})_2\text{PNNP}]$ (0.20 g, 0.184 mmol) in CH_2Cl_2 (5 mL) was treated with CH_3I (25.5 μL , 0.41 mmol). The resulting yellow solution decolorized over ~ 20 min with concomitant formation of an off-white precipitate. After 30 min, ether (50 mL in portions) was added and the product so obtained was recrystallized from CH_2Cl_2 /ether; 0.23 g (86%). This complex proved to be a mixture of three geometric isomers A–C in a ratio of $\sim 1:2:3$. ^1H NMR (200 MHz): δ 0.71 (dd, $J = 6.6, 3.9$ Hz, isomer A), 0.41 (dd, $J = 7.1, 4.4$ Hz, isomer B), 0.34 (dd, $J = 7.1, 4.6$ Hz, isomer C), 1.18 (t, $J = 7$ Hz, 6 H), 3.43 (q, $J = 7$ Hz, 4 H), 4.3–4.8 (m, 4 H), 6.3–6.4 (overlapping s, 1 H), 7.0–8.5 (m, 30 H). Anal. Calcd for $\text{C}_{45}\text{H}_{41}\text{I}_2\text{N}_2\text{O}_3\text{P}_3\text{Ir}_2 \cdot \text{C}_4\text{H}_{10}\text{O}$: C, 40.67; H, 3.55; I, 17.54; N, 1.94; P, 6.42. Found: C, 40.64; H, 3.43; I, 17.26; N, 1.97; P, 6.41.

Crystallographic Analysis of $[\text{Rh}_2(\mu\text{-PPh}_2)(\text{CO})_2\text{PNNP}(\text{CH}_3)\text{I}] \cdot \text{C}_4\text{H}_{10}\text{O}$. Crystals were obtained as orange-brown blocks from CH_2Cl_2 /ether. An approximately triangular shaped flake of dimensions $0.175 \times 0.175 \times 0.125 \times 0.125$ mm in the direction $[1,0,1]$, $[1,1,1]$, $[1,0,1]$, and $[0,1,1]$, respectively, was used throughout. Precession photographs were used to obtain preliminary cell and symmetry information. Further work was on an Enraf-Nonius CAD-4 diffractometer using graphite-monochromatized Mo K α radiation (λ 0.71069 Å).

Crystal Data: $\text{C}_{44}\text{H}_{37}\text{IN}_2\text{O}_3\text{P}_3\text{Rh}_2 \cdot \text{C}_4\text{H}_{10}\text{O}$, triclinic, space group $P1$ or $P\bar{1}$ ($P\bar{1}$ by successful analysis), $a = 12.211$ (4) Å, $b = 13.313$ (7) Å, $c = 15.616$ (7) Å, $\alpha = 79.34$ (5)°, $\beta = 72.64$ (3)°, $\gamma = 84.37$ (4)°, $V = 2379$ Å³, $D_{\text{calcd}} = 1.57$ g cm⁻³ for $Z = 2$; Mo K α radiation (λ 0.71069 Å), $\mu(\text{Mo K}\alpha) = 14.6$ cm⁻¹, $T = 300$ K.

Cell constants were obtained by least-squares refinement of the setting angles of 25 reflections ($9.6 < \theta < 15.9^\circ$). Intensity data were collected in the $\theta/2\theta$ mode with scan ranges of $(1.0 + 0.35 \tan \theta)^\circ$ within a maximum scan time of 80 s. All 9347 reflections in the quadrants ($h, \pm k, \pm l$) with $2\theta \leq 50^\circ$ were collected. Three standard reflections, which were monitored after every 8000 s of exposure time, showed no significant variations during data collection.

Lorentz and polarization corrections were applied to all data. Absorption corrections were not considered necessary since $\mu = 14.6$ cm⁻¹. Subsequent averaging of 1088 symmetry-equivalent reflections ($R_{\text{merge}} = 0.013$) and the rejection of 600 reflections with $F_o = 0.0$ gave a data set of 7885 reflections.

All three heavy atoms were located in the Patterson function, and subsequent cycles of least squares and Fourier calculations revealed all missing atoms in the molecule as well as the presence of the ether solvent in the lattice. In the final cycles, all hydrogen atoms with the exception of those associated with the CH_3 group were placed in calculated positions ($\text{C-H} = 0.95$ Å; $B = 7.5$ Å²) but were not refined. Full-matrix least-squares refinement minimizing $\sum w|F_o - |F_c||^2$ then converged

(maximum shift/error 0.20) to the agreement indices $R = 0.0401$ ($R_w = 0.0586$) for 6739 reflections with $I > 3\sigma(I)$. Weights in the final cycle were given by $w = 4F^2[\sigma(I)^2 + (0.035F^2)^2]^{-1}$, the esd of an observation of unit weight was 2.16, and a final difference Fourier was featureless. A PDP 11/23 computer and programs in the Enraf-Nonius SDP package²⁹ were used for the refinement.

Acknowledgment. This work was supported by grants from the Natural Sciences and Engineering Research Council of Canada who also awarded T.G.S. a scholarship.

(29) "Enraf-Nonius Structure Determination Package"; B. A. Frenz and Associates: College Station, TX, 1981.

Registry No. 1, 96532-16-0; 2-BF₄, 96532-18-2; 4-BF₄, 96532-20-6; 7, 96532-21-7; 8, 96532-22-8; 9, 96532-23-9; 10, 96532-24-0; 11, 96532-26-2; 12, 96532-27-3; 13, 96532-28-4; 14, 96532-29-5; 15, 96532-30-8; 16, 96532-31-9; CH₃COCl, 75-36-5; CH₃I, 74-88-4; Ir₂H₂(COD)₂PNNP*, 96555-14-5; PhCH=CH₂, 100-42-5; PhC≡CPh, 588-59-0; CH₂=C(CH₃)CH=CH₂, 78-79-5; CH₂=CHCOH, 107-02-8; CH₂=CHCH₂CH₂CH=CH₂, 592-42-7; PhCH₂CH₃, 100-41-4; *cis*-PhCH=CHPh, 645-49-8; *trans*-PhCH=CHPh, 103-30-0; PhCH₂CH₂Ph, 103-29-7; 1,3-cyclohexadiene, 592-57-4; 1,3-cyclooctadiene, 1700-10-3; benzene, 71-43-2; cyclohexane, 110-82-7.

Supplementary Material Available: Tables of hydrogen atom positions, general temperature factor expressions, bond distances and bond angles, and final structure factor amplitudes for 11 (45 pages). Ordering information is given on any current masthead page.

Contribution from the Department of Chemistry,
Ball State University, Muncie, Indiana 47306

Syntheses, Characterization, and Properties of Palladium(II) Complexes Containing Bidentate Phosphine-Nitrile or Phosphine-Imidate Ligands

MOHAMMAD HABIB, HOREB TRUJILLO, CATHERINE A. ALEXANDER, and BRUCE N. STORHOFF*

Received September 14, 1984

The reactions of H₂PdX₄ (X = Cl, Br) with Ph₂PCH₂CH(CH₃)CN, Ph₂P(CH₂)₂CN, or Ph₂P(*o*-C₆H₄CN) (L) in a 1.0:2.1 mole ratio yield the corresponding *trans*-PdX₂L₂ complexes in which the L groups function as monodentate phosphines. For the case in which L = Ph₂PCH₂CH(CH₃)CN, both ³¹P and ¹³C NMR measurements indicate the presence of approximately equal quantities of each diastereomer. For the latter two ligands, complexes of stoichiometry [LPdX₂]₂ are also readily obtained. For the Ph₂P(*o*-C₆H₄CN)-based dimers, IR and NMR data are consistent with halogen-bridged formulations. Similarly obtained data from the Ph₂P(CH₂)₂CN-containing dimers indicate the presence of more than one isomer. These data are rationalized on the basis of halogen-bridged and ligand-bridged dimers that interconvert rapidly on the NMR time scale. The nitrile groups in all the dimeric complexes react with alcohols (methanol and/or ethanol) to yield the corresponding chelated phosphine-imidate complexes.

Introduction

Bidentate ligands with two types of donor sites are well-known and have been the subject of many reports. Ligands of this general type are of interest because they can bridge dissimilar metals or, if one donor is easily replaced, yield complexes that readily provide a coordination site for incoming substrates.^{1,2} Included, for example, are phosphines that also contain a carbon,³ nitrogen,⁴⁻¹¹ oxygen,¹²⁻¹⁵ or sulfur¹⁶⁻¹⁸ donor atom. Of the nitrogen-containing

phosphines, 2-(diphenylphosphino)pyridine,⁴ 3-(diphenylphosphino)-*N,N*-dimethylpropylamine,^{6,7} 3-(diphenylphosphino)propionitrile,¹⁰ and *o*-(diphenylphosphino)benzotrile¹¹ are four examples that collectively function as both chelating and bridging ligands. The ligand properties of 2-(diphenylphosphino)pyridine are, in particular, well established and provide homonuclear and heteronuclear ligand-bridged dimers of diverse reactivities.^{4,19-22}

We have reported rhenium(I) complexes of the stoichiometry Re₂(CO)₆L₂X₂ (L = 3-(diphenylphosphino)propionitrile, *o*-(diphenylphosphino)benzotrile; X = Cl, Br).^{10,11} From spectroscopic data, we concluded that these complexes were ligand- rather than halogen-bridged dimers in which the nitrile groups coordinated in end-on fashion. As expected,² the nitrile groups in these complexes could be readily replaced by a variety of other donors. To further establish the nature of phosphine-nitrile ligands, we have now synthesized several palladium(II) complexes of 3-(di-

- (1) Davies, J. A.; Hartley, F. R. *Chem. Rev.* **1981**, *81*, 79.
- (2) Storhoff, B. N.; Lewis, H. C., Jr. *Coord. Chem. Rev.* **1977**, *23*, 1.
- (3) King, R. B.; Efraty, A. *J. Am. Chem. Soc.* **1971**, *93*, 564.
- (4) Farr, J. P.; Olmstead, M. M.; Balch, A. L. *J. Am. Chem. Soc.* **1980**, *102*, 6654.
- (5) Dagnac, P.; Turpin, R.; Poilblanc, R. *J. Organomet. Chem.* **1983**, *253*, 123.
- (6) Knebel, W. J.; Angelici, R. J.; Gansow, O. A.; Darensbourg, D. J. *J. Organomet. Chem.* **1974**, *66*, C11.
- (7) Roundhill, D. M.; Bechtold, R. A.; Roundhill, S. G. N. *Inorg. Chem.* **1980**, *19*, 284.
- (8) Issleib, K. *Phosphorus Sulfur* **1976**, *2*, 219.
- (9) Foxman, B. M.; Goldberg, P. L.; Mazurek, H. *Inorg. Chem.* **1981**, *20*, 4368.
- (10) Storhoff, B. N. *J. Organomet. Chem.* **1972**, *43*, 197.
- (11) Storhoff, B. N.; Infante, A. *J. Inorg. Chem.* **1974**, *13*, 3043.
- (12) Dombek, B. D. *J. Org. Chem.* **1978**, *43*, 3408.
- (13) Jeffrey, J. C.; Rauchfuss, T. B. *Inorg. Chem.* **1979**, *18*, 2658.
- (14) Emsall, H. D.; Shaw, B. L.; Turtle, B. L. *J. Chem. Soc., Dalton Trans.* **1976**, 1500.
- (15) Braunstein, P.; Fischer, J.; Matt, D.; Pfeffer, J. *J. Am. Chem. Soc.* **1984**, *106*, 410.

- (16) Roundhill, D. M.; Beaulieu, W. B.; Bagchi, U. *J. Am. Chem. Soc.* **1979**, *101*, 5428.
- (17) Morris, R. H.; Ressler, J. M.; Sawyer, J. F.; Shiralian, M. *J. Am. Chem. Soc.* **1984**, *106*, 3683.
- (18) Issleib, K.; Gans, W. Z. *Anorg. Allg. Chem.* **1981**, *475*, 116.
- (19) Farr, J. P.; Wood, F. E.; Balch, A. L. *Inorg. Chem.* **1983**, *22*, 3387.
- (20) Farr, J. P.; Olmstead, M. M.; Wood, F. E.; Balch, A. L. *J. Am. Chem. Soc.* **1983**, *105*, 792.
- (21) Maisonnnet, A.; Farr, J. P.; Olmstead, M. M.; Hunt, C. T.; Balch, A. L. *Inorg. Chem.* **1982**, *21*, 3961.
- (22) Farr, J. P.; Olmstead, M. M.; Hunt, C. H.; Balch, A. L. *Inorg. Chem.* **1981**, *20*, 1182.